

# Boundary layer emission and Z-track in the color-color diagram of luminous LMXBs

M.G. Revnivtsev<sup>1,2</sup>, M.R. Gilfanov<sup>1,2</sup>,

<sup>1</sup> Max-Planck-Institute für Astrophysik, Karl-Schwarzschild-Str. 1, D-85740 Garching bei München, Germany,

<sup>2</sup> Space Research Institute, Russian Academy of Sciences, Profsoyuznaya 84/32, 117997 Moscow, Russia

**Abstract.** Based on archival data of RXTE observations of five bright neutron star LMXBs we demonstrate that Fourier-frequency resolved spectra of atoll and Z- sources are identical, despite significant difference in their average spectra and luminosity (by a factor of  $\sim 10 - 20$ ). This result fits in the picture we suggested earlier, namely that the  $f \gtrsim 1$  Hz variability in luminous NS LMXBs is primarily due to variations of the boundary layer luminosity. In this picture the frequency resolved spectrum equals the boundary layer spectrum, which therefore can be straightforwardly determined from the data. The obtained so boundary layer spectrum is well approximated by the saturated Comptonization model, its high energy cut-off follows  $kT \approx 2.4$  keV black body. Its independence on the global mass accretion rate lends support to the theoretical suggestion by Inogamov & Sunyaev (1999) that the boundary layer is radiation pressure supported. With this assumption we constrain the gravity on the neutron star surface and its mass and radius. Equipped with the knowledge of the boundary layer spectrum we attempt to relate the motion along the Z-track to changes of physically meaningful parameters. Our results suggest that the contribution of the boundary layer to the observed emission decreases along the Z-track from conventional  $\sim 50\%$  on the horizontal branch to a rather small number on the normal branch. This decrease can be caused, for example, by obscuration of the boundary layer by the geometrically thick accretion disk at  $\dot{M} \sim \dot{M}_{\text{Edd}}$ . Alternatively, this can indicate significant change of the structure of the accretion flow at  $\dot{M} \sim \dot{M}_{\text{Edd}}$  and disappearance of the boundary layer as a distinct region of the significant energy release associated with the neutron star surface.

**Key words.** accretion, accretion disks – instabilities – stars:binaries:general – stars:neutron – X-rays:general – X-rays:binaries

## 1. Introduction

Accreting neutron stars in low mass X-ray binaries (LMXB) are among the most luminous compact X-ray sources in the Galaxy. At least several of them have luminosities exceeding  $\sim \text{few} \times 10^{38}$  erg/s and presumably accrete matter at the level close to the critical Eddington accretion rate. Early observations of these sources (e.g. Toor et al., 1970) revealed rather soft X-ray spectra, indicating that their X-ray emission is predominantly formed in the optically thick media. Similar to accreting black holes, at lower X-ray luminosities (lower mass accretion rates),  $L_x \lesssim 5 \times 10^{36}$  erg/s, neutron stars undergo a transition to the hard spectral state (e.g. Barret, 2001). The energy spectra in this state point at the low optical depth in the emission region.

In the soft spectral state, the commonly accepted picture of accretion at not too extreme values of accretion rate has two main ingredients – the accretion disk (AD) and the boundary layer (BL). While in the disk matter rotates with nearly Keplerian ve-

locities, in the boundary layer it decelerates down to the spin frequency of the neutron star and settles onto its surface. For the typical neutron star spin frequency ( $\lesssim 500 - 700$  Hz) comparable amounts of energy are released in these two regions (Sunyaev & Shakura, 1986; Sibgatullin & Sunyaev, 2000). This picture is based on rather obvious qualitative expectations as well as more sophisticated theoretical considerations and numerical modeling (Sunyaev & Shakura, 1986; Kluzniak, 1988; Inogamov & Sunyaev, 1999; Sibgatullin & Sunyaev, 2000). It has been receiving, however, little direct observational confirmation. Due to similarity of the spectra of the accretion disk and boundary layer the total spectrum has a smooth curved shape, which is difficult to decompose into separate spectral components (Mitsuda et al., 1984; White et al., 1988; Di Salvo et al., 2001; Done et al., 2002). This made application of physically motivated spectral models to the description of observed spectra of luminous neutron stars difficult, in spite of very significant increase in the sensitivity of X-ray instruments. A possible solution was suggested by early results of Mitsuda et al. (1984), which demonstrated the po-

tential of using the combined spectral and variability information.

Recently, Gilfanov, Revnivtsev & Molkov (2003) analyzed spectral variability in luminous LMXBs and showed that in these sources aperiodic and quasi periodic variability on  $\sim$  sec – msec time scales is caused primarily by variations of the luminosity of the boundary layer. Its spectral shape remains nearly constant in the course of the luminosity variations and is represented by the Fourier frequency resolved spectrum. Moreover, in the considered range  $\dot{M} \sim (0.1 - 1)\dot{M}_{\text{Edd}}$  ( $\dot{M}_{\text{Edd}}$  is the critical Eddington mass accretion rate) it depends weakly on the global mass accretion rate and in the limit  $\dot{M} \sim \dot{M}_{\text{Edd}}$  is close to Wien spectrum with  $kT \sim 2.4$  keV. Such a behavior is in accord with the predictions of the model by Inogamov & Sunyaev (1999), namely, that at sufficiently high accretion rates,  $\dot{M} > 0.1\dot{M}_{\text{Edd}}$ , the boundary layer is radiation pressure dominated and the local radiation flux is close to the critical Eddington value. Increase of the mass accretion rate leads to the increase of the emitting area of the BL, while its vertical structure changes little (Inogamov & Sunyaev, 1999).

In this paper we further explore the behavior of the boundary layer and the accretion disk emission in a number of bright neutron star LMXBs (both Z and atoll sources) and qualitatively describe their evolution with change of a mass accretion rate. We will concentrate on neutron star LMXBs in the soft/high spectral state with luminosities  $L_X \gtrsim 0.5 - 1 \times 10^{37}$  erg/s. Our study will be based on the results of Gilfanov, Revnivtsev & Molkov (2003), namely, that the shape of the boundary layer spectrum is adequately represented by the frequency resolved spectrum (energy spectrum of the variable part of the emission) at the Fourier frequencies above  $f \gtrsim 1$  Hz.

## 2. Data

For our study we used data of RXTE observatory (Bradt et al., 1993), which combines large collecting area with high time resolution. We have studied all Z-sources except for GX349+2 which during the majority of RXTE observations was on the “flaring” branch of its color-color diagram, supposedly corresponding to super-Eddington mass accretion rates (Hasinger & van der Klis, 1989). The behavior of sources at such high accretion rates is more complex and is beyond the scope of this paper. The remaining five Z sources are: Cyg X-2, GX340+0, Sco X-1, GX 5-1 and GX 17+2. For these sources we have excluded the time intervals corresponding to the “flaring” branch of their color-color diagram. The atoll sources were represented in our sample by 4U1608-52 and 4U1820-30 in their soft/high spectral state, showing high rapid flux variability.

For the data reduction we used standard programs of package HEASOFT 5.3 in accordance to the RXTE Guest Observer Facility recommendations. We have corrected the obtained energy spectra for the deadtime and the pile up effects (<http://lheawww.gsfc.nasa.gov/>

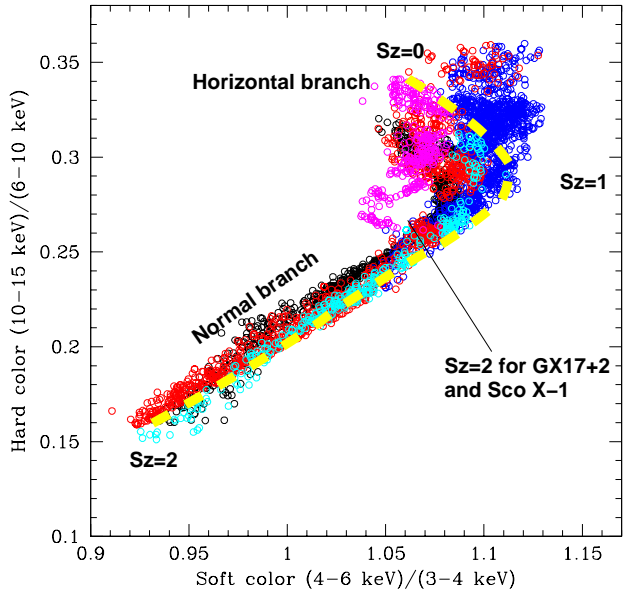


**Fig. 1.** Color-color diagram of all Z-sources except for GX349+2. Only horizontal and normal branch data are shown. Colors were calculated as ratios of absorption corrected energy fluxes in the following energy channels 3.0–4.0 keV, 4.0–6.0 keV, 6.0–10.0 keV, 10–15.0 keV. Dashed line shows the approximation to the Z-track by an arbitrary smooth curve. Turning points of the Z-track are marked with  $S_z = 0, 1, 2$

docs/xray/xte/pca/). All subsequent spectral approximations included interstellar absorption which was fixed at values :  $N_H = 6 \times 10^{22} \text{ cm}^{-2}$  for GX 340+0,  $0.2 \times 10^{22} \text{ cm}^{-2}$  for Cyg X-2,  $0.2 \times 10^{22} \text{ cm}^{-2}$  for Sco X-1,  $1.0 \times 10^{22} \text{ cm}^{-2}$  for GX 17+2,  $3.0 \times 10^{22} \text{ cm}^{-2}$  for GX 5-1,  $1.0 \times 10^{22} \text{ cm}^{-2}$  for 4U1608-52 and  $0.2 \times 10^{22} \text{ cm}^{-2}$  for 4U1820-30. The luminosities of all Z sources are approximately  $2 \times 10^{38} \text{ erg s}^{-1}$ , for 4U1608-52 and 4U1820-30 approximately  $10^{37} \text{ erg s}^{-1}$ .

The color-color diagrams (CCD) of these sources are presented in Fig.1. For construction of the CCDs we have used energy channels 2.0–4.0 keV, 4.0–6.0 keV, 6.0–10.0 keV and 10.0–15.0 keV. The hard and soft colors are ratio of energy fluxes of sources in abovementioned energy bands. Energy fluxes were computed from spectra averaged over 128 sec intervals. All fluxes were corrected for absorption.

## 3. Spectrum of the boundary layer

The frequency resolved spectra (the energy spectrum of the variable part of the emission, Revnivtsev et al. 1999) computed at the frequencies  $f \gtrsim 1 - 5$  Hz are shown for five sources from our sample in Fig.2. For Z sources we used only data on the horizontal branch of the CCD

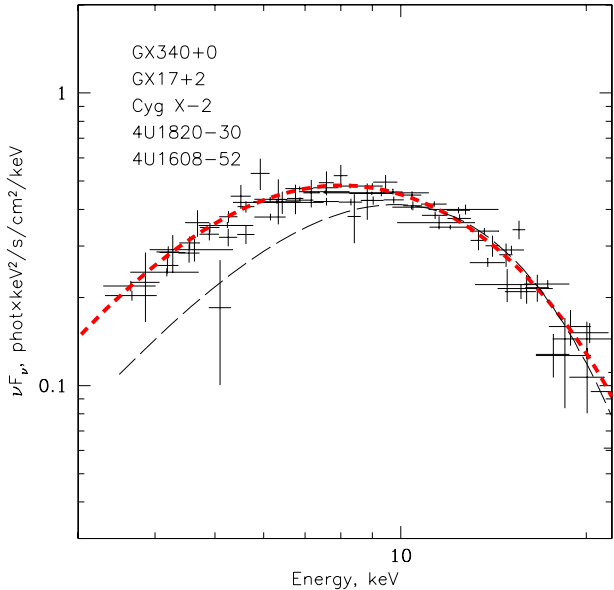


**Fig. 2.** Fourier-frequency resolved spectra ( $\approx$  boundary layer spectra) of sources from our sample. All spectra were corrected for the interstellar absorption. The thick dotted line shows the best fit Comptonization model with  $kT_s = 1.5$ ,  $kT_e = 3.3$  keV,  $\tau = 5$ . Thin dashed line shows the blackbody spectrum with temperature  $kT_{bb} = 2.4$  keV.

where the amplitude of variability at these frequencies is maximal. For Sco X-1 and GX 5-1 the RXTE archive does not contain high time resolution data for the horizontal branch with sufficient number of energy channels. The frequency resolved spectrum of 4U1608-52 was taken from Gilfanov, Revnivtsev & Molkov (2003). For plotting purposes, the normalizations of all spectra were adjusted to match that of GX340+0.

Similarity of the spectra shown in Fig.2 is remarkable, considering significant difference in the average spectra and a factor of  $\sim 10 - 20$  spread in the luminosity between atoll and Z-sources ( $\sim 0.1\dot{M}_{Edd}$  and  $\sim \dot{M}_{Edd}$  correspondingly). This behavior fits in the picture proposed by Gilfanov, Revnivtsev & Molkov (2003). As summarized in the Introduction, they showed, in particular, that the frequency resolved spectra at these frequencies equal the spectrum of the boundary layer emission.

The shape of the frequency resolved ( $\approx$  boundary layer) spectrum can be adequately described by the saturated Comptonization. For the sake of comparison with other results and for convenient parametrization of the BL spectrum we used the Comptonization model of Titarchuk (1994). The best fit parameters of the model fitted in the 3-20 keV range simultaneously to all five spectra shown in the Fig.2 are: temperature of seed photons  $kT_s = 1.5 \pm 0.1$ , temperature of electrons  $kT_e = 3.3 \pm 0.4$  and the optical

depth  $\tau = 5 \pm 1$  for slab geometry. The best fit model is shown by the thick dotted line on Fig.2. The temperature of the black body spectrum describing the shape of the cutoff in the observed spectrum at energies  $> 13$  keV is  $kT_{bb} = 2.4 \pm 0.1$  keV (thin dashed line on Fig.2).

It would be interesting to follow up on the results of Gilfanov, Revnivtsev & Molkov (2003) and to consider the evolution of the boundary spectrum along the Z track from the horizontal to normal branch. Unfortunately, apart from GX340+0, already considered in their paper, the variability level on the normal branch of color-color diagram for other four Z-sources is insufficient to obtain frequency resolved spectra with reasonable signal-to-noise ratio.

#### 4. Constraints on NS mass and radius from the BL spectrum

The independence of the spectrum of the boundary layer on the luminosity lends support to the theoretical predictions by Inogamov & Sunyaev (1999) that the boundary layer is radiation pressure supported, i.e. radiates at the local Eddington flux limit. In this picture, the parameters of the BL emission can be used to determine the value of the Eddington flux limit on the surface of the neutron star. As the Eddington flux limit is uniquely determined by the neutron star surface gravity and the atmospheric chemical composition, the neutron star mass and radius can be constrained.

If the boundary layer emitted true black body emission, the radiation flux of the unit area was determined only by its temperature. Therefore the observed shape of the BL spectrum, in particular the best fit black body temperature, could be used to determine the value of the Eddington flux limit on the neutron star surface. This approach has been utilized in the context of the Eddington limited X-ray bursts (e.g. Goldman, 1979; Marshall, 1982; Lewin, van Paradijs, & Taam, 1993; Titarchuk & Shaposhnikov, 2002). For fully ionized hydrogen atmosphere:

$$\frac{\sigma T^4}{c} \frac{\sigma_T}{m_p} = \frac{GM(1 - R_g/R)^{3/2}}{R^2}$$

where  $\sigma$  - Stefan-Boltzmann constant,  $\sigma_T$  - Thomson cross-section,  $T$  - black body temperature at infinity,  $m_p$  - proton mass,  $M$  - mass and  $R$  - radius of the neutron star,  $R_g = 2GM/c^2$  - gravitational radius of the neutron star. In addition, one would have to take into account that the value of the Eddington flux is somewhat (by  $\sim 10 - 20\%$ ) reduced because of the action of the centrifugal force (Inogamov & Sunyaev, 1999).

In reality, scatterings are important in the atmosphere of the neutron star, therefore, the boundary layer spectrum will differ from the black body (e.g. London, Howard, & Taam 1986; Lewin, van Paradijs, & Taam 1993). The radiation transfer problem in the atmosphere of the neutron star has

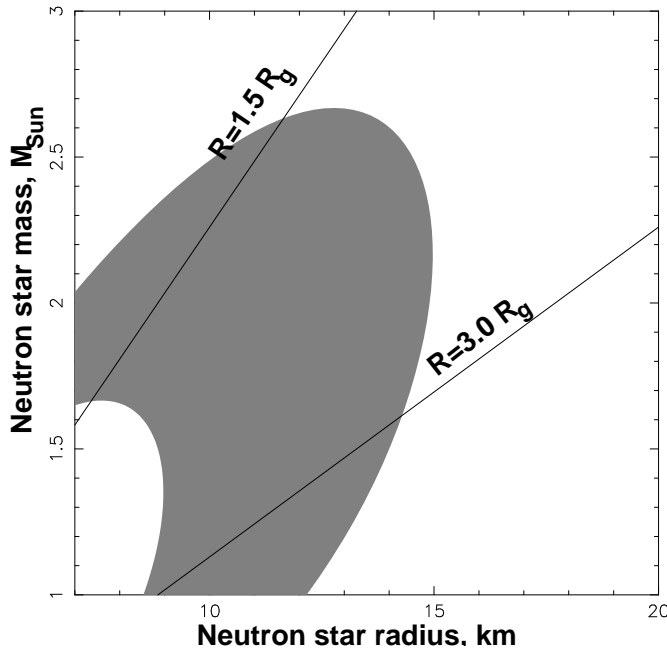


**Fig. 3.** Constraints on the mass and radius of the neutron star in bright LMXBs. Solid lines denote the regions where neutron star radius  $R$  equals to  $1.5R_g$  (radius of photon orbit in Schwarzschild metric) and  $3.0R_g$  (radius of last stable orbit of an accretion disk in Schwarzschild metric)

been intensively investigated, in particular in the context of X-ray bursts. Numerical calculations show that the effects of scatterings can be approximately accounted for by introducing the spectral hardening factor which relates the color and the effective temperatures of the emission (Syunyaev & Shakura, 1974; London, Howard, & Taam, 1986; Titarchuk, 1994; Shimura & Takahara, 1995; Ross & Fabian, 1996). Typical values of the hardening factor are about  $\sim 1.7$ . We used this result in order to make simple estimates of the gravity on the neutron star surface and to constrain its mass and radius. In these calculations we assumed the color temperature of the boundary layer emission  $T = 2.4$  keV and considered the range of the hardening factor values of 1.6-1.8. We assumed that the centrifugal force reduces the Eddington flux limit in comparison with non-rotating boundary layer by 20%. We also took into account the finite height of the boundary/spreading layer, about 1 km (Inogamov & Sunyaev, 1999). The calculations were performed for Schwarzschild geometry, hydrogen atmosphere. The result is shown in Fig.3. The width of the shaded region is defined by the assumed range of the values of the hardening factor.

Finally we note that the similarity of the spectral shape of the BL spectrum in different sources (Fig.2) indicates that they have close values of the mass and radius, in particular, that there is no significant difference in the surface gravity between atoll and Z-sources. It also shows that there are no significant differences caused by variations in the atmospheric chemical abundances between sources.

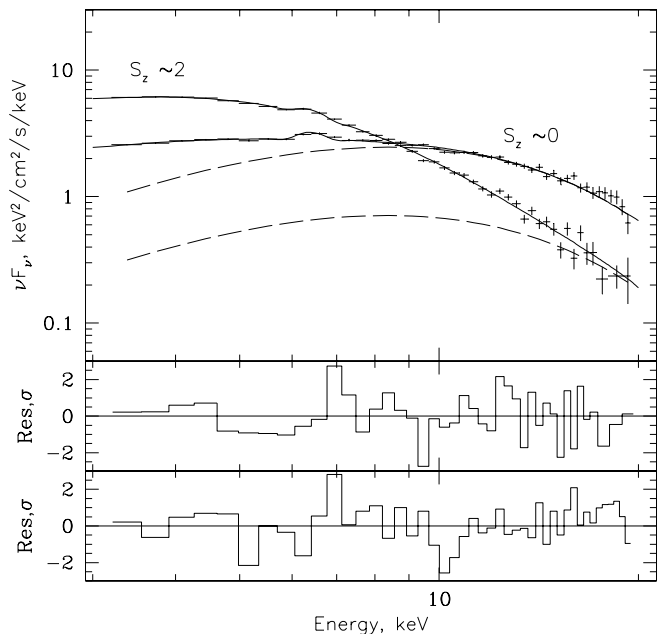


**Fig. 4.** Spectra of Cyg X-2 at the beginning of horizontal branch ( $S_z \sim 0$ ) and at the end of the normal branch ( $S_z \sim 2$ ). Solid lines are best fit models of the spectra. Dashed lines denote the boundary layer components

In particular we did not find statistically significant difference between ultracompact compact binary 4U1820-30 and other sources.

## 5. Evolution along Z-track

In order to study the behavior of Z-sources in the color-color diagram we consider their spectra integrated over 128-sec time intervals. These spectra are fitted with a simple model consisting of two components, representing contributions of the boundary layer and the accretion disk. Also included in the model was the gaussian line at the energy 6.4 keV. It is not energetically important but significantly improves quality of the fit. The line parameters will not be considered here. The shape of the boundary layer spectrum was approximated by comptt model with the best fit parameters obtained in the section 3. For the accretion disk spectrum we adopt the multicolor disk blackbody Shakura & Sunyaev (1973); Mitsuda et al. (1984) (*diskbb* model in XSPEC fitting package).

Quality of the spectral fits is uniformly good on the horizontal and normal branches of the Z-track in the color-color diagram, with the reduced  $\chi^2$  never exceeding  $\sim 1.3$  for 41 degrees of freedom. Relative deviations of the model from the data does not exceed approximately one percent. This is illustrated by Fig.4, showing two spectra of Cyg X-2, at the beginning of the horizontal branch and at the end of the normal branch.

The model is obviously oversimplified. Firstly, it relies on the assumption about the shape of the boundary layer spectrum. This seems to have been established rather

well for the horizontal branch and for the upper part of the normal branch. For the latter, it has been shown for GX340+0 only, for other sources the signal-to-noise ratio being insufficient. On the lower part of the normal branch the variability level and, consequently the signal-to-noise ratio of the frequency resolved spectra, are too low to conduct a similar study for any of the sources in our sample. Secondly, we chose the diskbb model to represent the spectrum of the accretion disk. Although the model involves several well known simplifying assumptions it has been shown to approximately reproduce the shape of the spectrum of the geometrically thin, optically thick accretion disk (Merloni, Fabian & Ross, 2000). The best fit color temperature obtained in this model can be related with certain accuracy to the maximum disk temperature. Therefore with this model we should be able to separate the disk and boundary layer components and to estimate their respective fluxes, as well as the characteristic temperature in the inner disk. Keeping in mind the limitations of the spectral model we will attempt to relate the motion of a source along the Z-track to the changes in the values of the physically meaningful parameters. The most important difference of our approach from similar studies undertaken previously is in a priori knowledge of the shape of the boundary layer spectrum.

### 5.1. Accretion disk

The relation between the accretion disk temperature and its flux for all five Z-sources is shown in Fig.5 (we emphasize that plotted along the x-axis is the disk flux, as opposite to the total flux). For three of them (GX 5-1, Cyg X-2 and GX 340+0) the disk temperature on the horizontal branch approximately follows the  $T \propto F_{\text{disk}}^{1/4}$  law, which is to be expected for a standard accretion disk. For Sco X-1 and GX17+2 the temperature increases with the disk flux faster than the  $T \propto F_{\text{disk}}^{1/4}$  law. For all sources the monotonic relation between the disk temperature and the disk flux breaks down on the normal branch and further along the Z-track the temperature either remains constant or decreases with the disk flux.

The significant deviation from  $T \propto F_{\text{disk}}^{1/4}$  law near the transition from the horizontal to the normal branch indicates that the simple accretion disk model in the form represented by xspec's diskbb becomes inapplicable. The exact reason for this is not clear. It may happen due to rather small modifications to the model, e.g. violation of the assumption that the effect of Comptonization can be represented by the single value of the spectral hardening factor, constant over the extend of the inner disk as well as along the Z-track in the color-color diagram. Alternatively, this might be an indication of the more significant break down of the standard geometrically thin, optically thick picture of the accretion disk. This would point at the significant modification of the structure and geometry of the accretion flow near the transition from the horizontal to the normal branch, presumably corresponding to  $\dot{M} \sim \dot{M}_{\text{Edd}}$ .

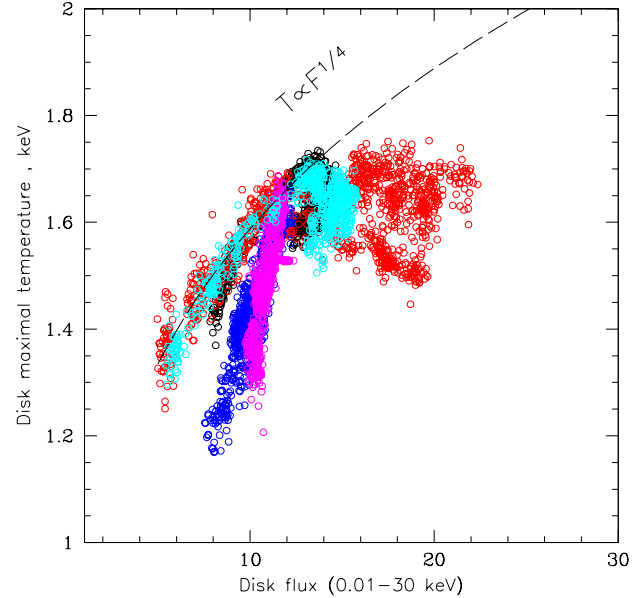


**Fig. 5.** Dependence of the disk temperature on its flux for five Z-sources. The units of flux are  $10^{-9}$  erg/s/cm $^2$ . Regions corresponding to the horizontal and normal branches are marked. Dashed curved line shows  $T \propto F_{\text{disk}}^{1/4}$  dependence. For GX5-1, GX340+0, GX 17+2 and Sco X-1 the flux values were scaled down by the factor of 1.3, 1.4, 1.4 and 13 respectively to match Cyg X-2 points at the end of the horizontal branch

Knowledge of the boundary layer and the accretion disk spectra allows one to (crudely) estimate the scale-height of the disk  $H/R$  in the region of the main energy release. Indeed, for the radiation pressure supported accretion disk its height is determined by the equality of the radiation pressure and the gravitational force (see e.g. Shakura & Sunyaev, 1973). For geometrically thin accretion disk the gravitational force near the neutron star is  $\sim R/H$  times smaller than on the neutron star surface. Assuming that the radiation transfer conditions are similar in the disk and in the boundary layer (i.e. the color hardening factors are similar, see section 4) we find  $H/R \sim (T_{\text{disk}}/T_{\text{BL}})^4 \sim 0.1 - 0.2$  which is comparable with the predictions of the simple disk theory for  $\dot{M} \sim \dot{M}_{\text{Edd}}$  (Shakura & Sunyaev, 1973, 1976). On the other hand, this estimate can be considered as a crude consistency check for the obtained values of the boundary layer and disk temperatures.

### 5.2. Boundary layer

The dependences of the BL contribution to the total X-ray emission on the position on the Z-track are plotted in Fig.6. The coordinate along the Z-track was defined to be

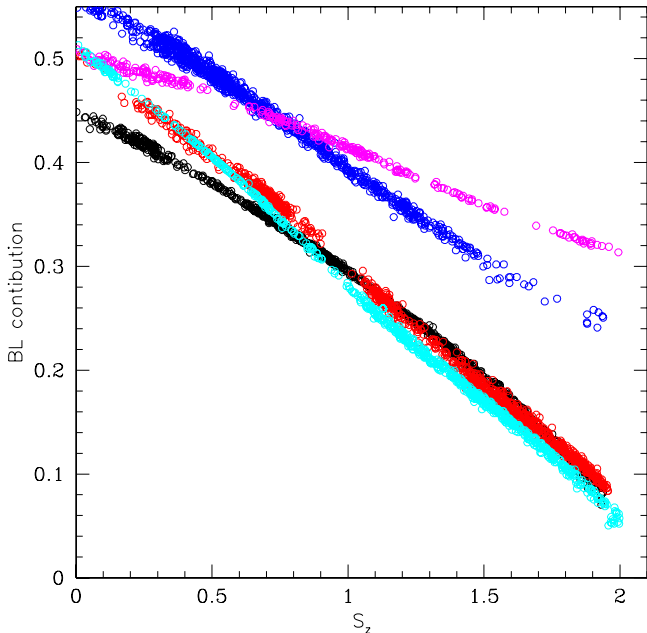


**Fig. 6.** Dependence of the boundary layer contribution to the total X-ray emission of Z sources as a fraction of the position on their Z-diagrams

proportional to the hard color with the reference points  $S_Z = 0, 1, 2$  defined as shown in Fig.1.

Statistical uncertainties in the values of the BL fraction are small and can be neglected, as confirmed by the dispersion of the points in Fig.6. More important are the systematic ones associated with the imprecise knowledge of the shape of the BL spectrum and its possible variations along the Z-track. In order to probe the amplitude of these uncertainties on the horizontal branch we explored the range of  $1\sigma$  errors of the parameters of the comptt model obtained in the section 3. The associated change of the boundary layer fraction did not exceed  $\approx 0.05 - 0.07$  in the units of Fig. 6. As for the normal branch, there is some difference between the frequency resolved spectra of GX340+0 on the horizontal and normal branch, the latter being better described by the Wien spectrum with  $kT=2.4$  keV than by the spectrum of saturated Comptonization (cf. thick and thin dashed lines in Fig.2). This difference could be related to weak dependence of the boundary layer spectrum on the global mass accretion rate (Gilfanov, Revnivtsev & Molkov, 2003). Substitution of the comptt model by the blackbody or Wien spectrum with  $kT = 2.4$  keV, decreases the boundary layer fraction by  $\approx 0.1$ . As it is clear from these numbers, systematic uncertainties might change the Fig.6 in details but does not affect the general trend in a significant way.

The Fig.4 and 6 suggest that the boundary layer fraction decreases along the Z-track and it is smaller on the normal branch than on the horizontal branch. As demonstrated above, this conclusion is rather robust, as long as the assumption regarding the constancy of the boundary layer spectrum is approximately correct. Even if the

diskbb model is not applicable on the normal branch any more, the  $\sim 5$ -fold decrease of the  $E \gtrsim 15$  keV flux between  $S_z = 0$  and  $S_z = 2$  effectively constrains the boundary layer contribution on the normal branch (Fig.6). As the variability at  $f \gtrsim 1$  Hz is primarily associated with the boundary layer emission, the decrease of the boundary layer fraction along the Z-track also explains well-known decrease of the level of aperiodic and quasi-periodic variability.

Although no complete physical interpretation of the observed behavior can be offered, we mention several possibilities. One of these is that the general structure of the accretion flow does not change significantly and  $\sim 50\%$  of the energy is always released on, or very close to the neutron star surface. The apparent decrease of the boundary layer fraction on the normal branch is a result of its geometrical obscuration by, for example, the geometrically thickened accretion disk. An alternative possibility is that at high values of the mass accretion rate  $\dot{M} \sim \dot{M}_{\text{Edd}}$  a significant modification of the accretion flow structure might occur and its division into two geometrically distinct parts – boundary layer and accretion disk, might become inapplicable. Namely, due to non-negligible pressure effects the deceleration of the orbital motion of the accreting matter from Keplerian frequency to the neutron star spin frequency would take place in a geometrically extended region with the radial extend of  $\Delta R \sim R_{\text{NS}}$ . In this case, the observed decrease of the boundary layer fraction could reflect actual decrease of the fraction of the energy released on the neutron star surface with the rest of the energy being released in the extended transition region. Finally, it is also possible that the apparent decrease of the boundary layer fraction as well as the peculiar behavior of the accretion disk temperature (Fig.5) is the consequence of the complete break down of the model on the normal branch of the color-color diagram.

Sco X-1 and GX17+2 appear to have higher boundary layer fraction at the end of the normal branch than other three sources. Another indication of the possibly higher contribution of the BL emission at  $S_z \sim 2$  in Sco X-1 and GX17+2 is that they typically show stronger fast variability at the normal and flaring branch than Cyg X-2, GX340+0 and GX5-1 (cf. Sco X-1 -like and Cyg X-2 -like sources, Hasinger & van der Klis, 1989; Kuulkers et al., 1994; Jonker et al., 2000; Piraino, Santangelo, & Kaaret, 2002; Homan et al., 2002). The observed difference can be caused, for example, by different inclination angles in these systems, as indicated by optical data (Fomalont, Geldzahler, & Bradshaw, 2001; Steeghs & Casares, 2002; Crampton & Cowley, 1976; Kuulkers et al., 1994). It should be mentioned though, that the appearance of the Fig.6 is a direct consequence of the definition of the  $S_z$  coordinate, in particular the definition of the  $S_z = 2$  reference point as the turning point from the normal to the flaring branch. If, for example, the BL fraction would be plotted against the hard color, all five sources will be almost indistinguishable.

### 5.3. Shape of Z-diagram

Motivated by these results we use the two-component spectral model introduced in the beginning of this section to explain behavior of the Z-sources on the color-color diagram. Unlike before, for the accretion disk spectral component we adopt here the general relativistic accretion disk model by Ebisawa et al. (1991) (the *grad* model in the XSPEC fitting package) which explicitly includes dependence on the mass accretion rate. The mass of the compact object and binary system inclination were fixed at  $M_{\text{NS}} = 1.4M_{\odot}$  and  $i = 60^\circ$ . Using this two-component spectral model we can calculate the position in the color-color diagram as a function of the mass accretion rate and the boundary layer fraction. This simple model is an attempt to understand general tendencies of the Z-diagram, rather than to construct its precise quantitative description. In particular, the fact is ignored, that the relation between the accretion disk temperature and its flux is more complex than predicted by the standard model of the geometrically thin disk (Fig.5).

The results are presented in Fig.7. The two dashed curves in the figure show the evolution of spectral colors with the increase of the mass accretion rate of the disk component for two different values of the boundary layer fraction. The upper curve assumes the BL-to-disk flux ratio of 0.8, in the lower curve the BL fraction equals zero. On each curve positions where the mass accretion rate equals  $\dot{M} = 0.5, 1, 2, 3, 4 \times 10^{18} \text{ g/s}$  are marked. The evolution of colors assuming a rapid change of the BL contribution from  $F_{\text{BL}}/F_{\text{disk}} = 0.8$  to zero approximately at  $\dot{M} = 2 \times 10^{18} \text{ g/s}$  is shown by thick solid line.

The general shape of the Z-track can be reproduced in the model as a result of variation of two parameters – the mass accretion rate and BL fraction. The mass accretion rate increases along the Z-track. The Z-shape of the track is defined by the variation of the BL fraction, which decreases along the normal branch from the value of  $\sim 50\%$  expected in the “standard” theories to a small number of the order of  $\sim 0$  at the end of the normal branch. Quantitatively, the exact value of the  $\dot{M}$ , corresponding to the transition from the horizontal to the normal branch depends on the disk model (*grad*) parameters – the binary system inclination, the mass of the neutron star and the spectral hardening factor. For our choice of parameters, it equals  $\dot{M} \sim 2 \cdot 10^{18} \text{ g/sec}$ , i.e. is of the order of the Eddington critical value for a  $1.4M_{\odot}$  neutron star, when we can expect that the structure of the inner accretion flow can start to change.

The location of the horizontal branch on the color-color diagram depends on the boundary layer fraction at smaller  $\dot{M}$ . Theoretically, it could be used to determine the latter from observations which would be of great help for the theory. In particular, our spectral model suggests  $F_{\text{BL}}/F_{\text{AD}} \sim 0.8$ . In practice, however, the direct comparison of this number with theoretical predictions for the energy release in the disk and boundary layer is complicated, because the observed flux ratio  $F_{\text{BL}}/F_{\text{disk}}$  is modi-

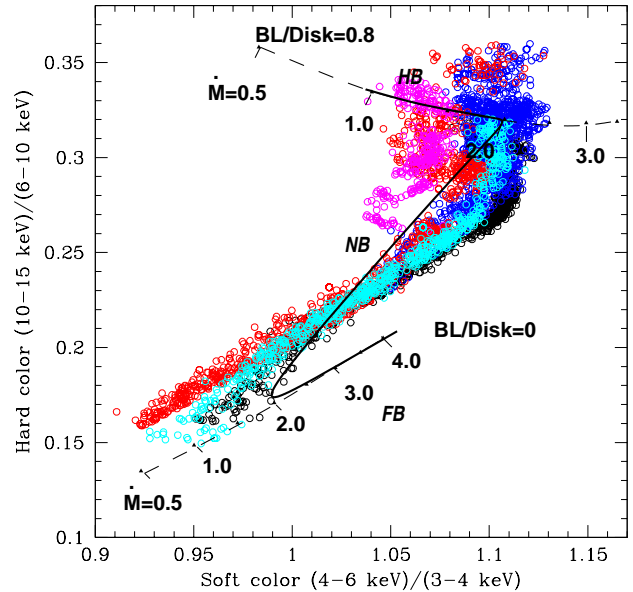


**Fig. 7.** The color-color diagram of 5 Z-sources. Overlayed on the data are the tracks predicted by the model (section 5.3). The thick two dashed lines show evolution of the colors with change of the accretion rate in the disk for two different values of the BL fraction: 44% (upper) and zero (lower). The values of the mass accretion rates  $\dot{M}$  of the disk component are marked in units of  $10^{18} \text{ g/s}$ . The thick solid line shows the Z track with transition mass accretion rate  $2 \times 10^{18} \text{ g/s}$ .

fied by geometrical factors and anisotropy of the AD and BL emission diagrams.

## 6. Summary

Using the archival data of RXTE observations of several bright LMXBs we study the boundary layer emission and the structure of the accretion flow in this sources. Our sample includes 2 atoll sources in the soft spectral state and 5 (all but one) Z-sources. Their luminosities range from  $\sim 10^{37} \text{ erg/s}$  (atoll sources) to  $\sim 2 \cdot 10^{38} \text{ erg/s}$  (Z-sources). Our results are summarized below.

– We construct Fourier-frequency resolved spectra (energy spectra of variable emission) at  $f \gtrsim 1 - 5 \text{ Hz}$  for five sources, which data combines sufficient timing and spectral resolution. Within the statistical uncertainties all the spectra have the same shape (Fig.2). This is a remarkable result as the average spectra of the atoll and Z-sources differ significantly and their luminosities range from  $\sim 10^{37} \text{ erg/s}$  (atoll sources) to  $\sim 2 \cdot 10^{38} \text{ erg/s}$  (Z-sources).

This result fits in the picture suggested by Gilfanov, Revnivtsev & Molkov (2003) and briefly

outlined in the Introduction. This picture implies, in particular, that the frequency resolved spectrum equals the energy spectrum of the boundary layer emission. The following is based on this assumption.

- The boundary layer spectrum in atoll sources and on the horizontal branch of Z-sources (i.e. at presumably sub-Eddington accretion rates) can be approximated by the spectrum of saturated Comptonization (section 3). Its high energy ( $E > 10$  keV) cut-off corresponds to the black body spectrum with temperature of  $kT \sim 2.4$  keV (Fig.2).
- Assuming that the boundary layer is radiation pressure supported we constrain the neutron star mass and radius. For a  $1.4M_{\odot}$  neutron star and the spectral hardening factor of 1.6–1.8 the NS radii are in the range of  $R_{\text{NS}} \sim 9 - 14$  km (Fig.3).
- We attempt to relate the motion of Z-sources along the Z-track to changes in the values of the physically meaningful parameters. Our results tentatively suggest that the contribution of the boundary layer component to the observed emission decreases along the Z-track from the conventional value of  $\sim 50\%$  on the horizontal branch to a rather small number at the end of the normal branch. The main difference of our approach from previous attempts is in the apriori knowledge of the shape of the boundary layer spectrum. This allowed us to avoid ambiguity of the spectral decomposition into boundary layer and disk components.

*Acknowledgements.* Authors thank Rashid Sunyaev, Nail Inogamov, Eugene Churazov, Juri Poutanen and Valery Suleimanov for useful discussions. This research has made use of data obtained through the High Energy Astrophysics Science Archive Research Center Online Service, provided by the NASA/Goddard Space Flight Center.

## References

Barret D., 2001, *AdSpR*, 28, 307

Bhattacharyya, S., Bhattacharya, D., Thampan, A. 2001, *MNRAS*, 325, 989

Bradshaw C. F., Geldzahler B. J., Fomalont E. B., 2003, *ApJ*, 592, 486

Bradt, H., Rotshild, R., Swank, J. 1993, *Astron. Astrophys. Suppl. Ser.* 97, 355

Crampton D., Cowley A. P., 1976, *ApJ*, 207, L171

Dieter, S., Vaughan, B., Kuulkers, E. et al. 2000, *A&A*, 353, 203

Di Salvo, T., Robba, N., Iaria, R. et al. 2001, *ApJ*, 554, 49

Done, C., Zyci, P. T. & Smith, D. A. 2002, *MNRAS*, 331, 453

Ebisawa, K., Mitsuda, K. & Hanawa, T. 1991, *ApJ*, 367, 213

Fomalont E. B., Geldzahler B. J., Bradshaw C. F., 2001, *ApJ*, 558, 283

Gilfanov, M., Churazov, E., Revnivtsev, M. 2000, *MNRAS*, 316, 923

Gilfanov, M., Revnivtsev, M., & Molkov, S. 2003, *A&A*, 410, 217

Gilfanov, M., Arefiev V. 2005, submitted to *MNRAS*, *astro-ph/0501215*

Goldman I., 1979, *A&A*, 78, L15

Grebenev, S. & Sunyaev, R. 2002, *Astronomy Letters*, 28, 150

Hasinger, G., van der Klis, M. 1989, *A&A*, 225, 79

Homan J., van der Klis M., Jonker P. G. et al. 2002, *ApJ*, 568, 878

Inogamov, N. & Sunyaev, R. 1999, *Astr.Lett*, 25, 269

Jonker, P., van der Klis, M., Wijnands, R. et al. 2000, *ApJ*, 537, 374

Kluzniak, W. 1988, PhD Thesis

Kuulkers E., van der Klis M., Oosterbroek T., Asai K., Dotani T., van Paradijs J., Lewin W. H. G., 1994, *A&A*, 289, 795

Lewin, W., Lubin, L., Tan, J. et al. 1992, *MNRAS*, 256, 545

Lewin W. H. G., van Paradijs J., Taam R. E., 1993, *SSRv*, 62, 223

London R. A., Howard W. M., Taam R. E., 1986, *ApJ*, 306, 170

Magdziarz, P. & Zdziarski, A.A. 1995, *MNRAS*, 273, 837

Marshall H. L., 1982, *ApJ*, 260, 815

Mendez, M., van der Klis, M., van Paradijs, J. et al. 1997, *ApJ*, 485, 37

Mendez, M., van der Klis, M., Ford, E. et al. 1999, *ApJ*, 511, 49L

Mendez, M., van der Klis, M., Ford, E. 2001, *ApJ*, 561, 1016

Miller, M. C., Lamb, F., Psaltis, D. 1998, *ApJ*, 508, 791

Mitsuda, K., Inoue, H., Koyama, K. et al. 1984, *PASJ*, 36, 741

Mitsuda, K. & Tanaka, Y., In: *The evolution of galactic X-ray binaries; Proceedings of the NATO Advanced Research Workshop*, Rottach-Egern, D. Reidel Publishing Co., 1986, p. 195.

Mitsuda, K. 1988, *AdSpR*, 8, 391

Piraino S., Santangelo A., Kaaret P., 2002, *ApJ*, 567, 1091

Popham, R. & Sunyaev, R. 2001, *ApJ*, 547, 355

Psaltis D., Lamb F. K., Miller G. S., 1995, *ApJ*, 454, L137

Revnivtsev, M., Gilfanov, M. & Churazov, E. 1999, *A&A*, 347, 23

Revnivtsev, M., Gilfanov, M., Churazov, E., Sunyaev, R. 2001, *A&A*, 372, 138

Ross, R. & Fabian, A. 1996, *MNRAS*, 281, 637

Schulz N. S., Wijers R. A. M. J., 1993, *A&A*, 273,

Shakura, N.I. & Sunyaev, R.A. 1973, *A&A*, 24, 337

Shakura N. I., Sunyaev R. A., 1976, *MNRAS*, 175, 613

Shakura, N.I. & Sunyaev, R.A. 1988, *Ad.Sp.R.*, 8, 135

Shimura, T. & Takahara, F. 1995, *ApJ*, 331, 780

Sibgatullin, N. & Sunyaev, R. 2000, *Astr.Lett.*, 26, 699

Steeghs D., Casares J., 2002, *ApJ*, 568, 273

Strohmayer, T. 2002, *Ad.Sp.R.*, 28, 511

Sunyaev R. A., Shakura N. I., 1974, *SvA*, 18, 60

Sunyaev, R. & Shakura, N. 1986, *SvAL*, 12, 117

Sunyaev, R. & Titarchuk, L., 1980, *A&A*, 86, 121

Tanaka, Y. & Shibazaki, N. 1996, ARA&A, 34, 607  
Titarchuk, L. 1994, ApJ, 429, 340  
Titarchuk L., Shaposhnikov N., 2002, ApJ, 570, L25  
Toor A., Seward F. D., Cathey L. R., Kunkel W. E., 1970,  
ApJ, 160, 209  
van der Klis, M. 1986, Lecture Notes in Physics, 266, 157  
van der Klis, M. 2000, ARA&A, 38, 717  
van der Klis, M. 2001, ApJ, 561, 934  
Vaughan, B., van der Klis, M., Lewin, W. et al. 1994, ApJ,  
421, 738  
Vaughan, B., van der Klis, M., Lewin, W. et al. 1999,  
A&A, 343, 197  
Vrtilek S. D., Raymond J. C., Garcia M. R., Verbunt F.,  
Hasinger G., Kurster M., 1990, A&A, 235, 162  
White, N., Stella, L., Parmar, A. 1988, ApJ, 324, 363